Poly-ε-caprolactone composite scaffolds for bone repair

R. DI LIDDO[1], P. PAGANIN[1], S. LORA[2], D. DALZOPPO[1], C. GIRAUDO[3], D. MIOTTO[3], A. TASSO[1], S. BARBON[2], M. ARTICO[4], E. BIANCHI[4], P.P. PARNIGOTTO[2], M.T. CONCONI[1] and C. GRANDI[1]

[1]Department of Pharmaceutical and Pharmacological Sciences, University of Padua, 35131 Padua; [2]Foundation for Biology and Regenerative Medicine, Tissue Engineering and Signalling (TES), Onlus, 35030 Padua; [3]Department of Medicine, University of Padua, 35128 Padua; [4]Department of Sensory Organs, University 'La Sapienza', 00161 Rome, Italy

Received July 18, 2014; Accepted September 3, 2014

DOI: 10.3892/ijmm.2014.1954

Abstract. Synthetic biomaterials combined with cells and osteogenic factors represent a promising approach for the treatment of a number of orthopedic diseases, such as bone trauma and congenital malformations. To guarantee optimal biological properties, bone substitutes are prepared with a 3D structure and porosity grade functional to drive cell migration and proliferation, diffusion of factors, vascularization and cell waste expulsion. In this study, synthetic hydroxyapatite (HA) or rat bone extracellular matrix (BP) were examined in an effort to optimize the mechanical properties and osteogenic activity of poly-ε-caprolactone scaffolds prepared with alginate threads (PCL-AT). Using rabbit bone marrow-derived mesenchymal stem cells (rMSCs), the effects of PCL composite substrates on cell adhesion, growth and osteogenic differentiation were evaluated. Micro-CT analysis and scanning electron microscopy evidenced that porous PCL scaffolds containing HA or BP acquire a trabecular bone-like structure with interconnected pores homogenously distributed and are characterized by a pore diameter of approximately 10 μm (PCL-AT-BP) or ranging from 10 to 100 μm. Although the porosity grade of both PCL-AT-HA and PCL-AT-BP promoted optimal conditions for the cell growth of rMSCs at the early phase, the presence of BP was crucial to prolong the cell viability at the late phase. Moreover, a precocious expression of Runx2 (at 7 days) was observed in PCL-AT-BP in combination with osteogenic soluble factors suggesting that BP controls better than HA the osteogenic maturation process in bone substitutes.

Introduction

Advanced bone surgical therapies are currently based on reconstruction surgery and tissue transplantation. However, several therapeutic and methodological limitations, such as the incomplete restoration of biological tissue functionality or the progressive deterioration of implants have been observed (1). As an alternative clinical approach, tissue engineering (2) has been suggested and is currently used to restore tissue damage, promoting the proliferation and differentiation of bone cells within synthetic scaffolds. In particular, cell-induced bone regeneration therapy is based on the transplantation of mesenchymal stem cells (MSCs) combined with biomaterials favouring an efficient diffusion of nutrients, a good gas exchange and 3D structure simulating *in vivo* local environment. The low grafting rate of engineered bone substitutes has been demonstrated to be greatly dependent on the porosity grade and geometry of the scaffold (1). As previously demonstrated by Langer and Vacanti (3), porous biomaterials enhance the therapeutic efficacy of cellular transplants, preserving cells from excretion and death. Synthetic and natural materials, such as polymers, ceramics, metals or their composites, have been largely investigated and their use has been explored for bone repair applications using *in vitro* and *in vivo* settings (2). Polymers, including collagen, hydroxyapatite (HA), polylactic acid (PLA), polyglycolic acid (PGA) and poly-ε-caprolactone (PCL) have been used to obtain biodegradable and mechanically resistant matrices using solution casting techniques (4), solvent casting particulate leaching (5), gel casting (6), gas saturation (7) and phase separation (8,9).

The success of biomaterials to sustain a complete bone repair is dependent on their ability to mimic the natural extracellular matrix (ECM), thereby minimizing foreign body or fibrotic responses. The mature bone matrix is composed of 65% minerals predominantly including HA and 35% protein (10) as collagen I (Coll I) fibers and proteoglycans (11). Bone ECM components act as primary chemical effectors in cell signaling and functionality. When HA (12,13) and/or Coll I (14,15) are combined with synthetic scaffolds such as PCL, matrices become highly osteoconductive (16) and acquire tensile and bending force, but no compressive strength. PCL is a semi-crystalline, aliphatic polyester with a degradation grade rate lower than collagen and strong mechanical strength (17). A composite matrix containing ECM and PCL has been previously investigated by Phipps *et al* (18) to obtain a useful scaffold with defined mechanical properties and a high level of biocompatibility. A tri-component electrospun scaffold

Correspondence to: Dr Rosa Di Liddo, Department of Pharmaceutical and Pharmacological Sciences, University of Padua, Via Marzolo, 5, 35100 Padua, Italy
E-mail: rosa.diliddo@unipd.it

Key words: poly-ε-caprolactone, composite scaffolds, bone extracellular matrix, mesenchymal stem cells, osteogenic differentiation

composed of PCL, Coll I and nanoparticulate HA was shown to blend the advantageous mechanical resistance of PCL with the favourable biochemical cues provided by native bone molecules, such as Coll I and HA, guaranteeing the better adhesion, spreading and proliferation of human MSCs (18).

In our previous study (9), experimental conditions were defined to obtain porous PCL scaffolds using the phase separation technique and alginate threads as porogen agents (PCL-AT). Although it was demonstrated to sustain osteoblastic adhesion, growth and differentiation, the mechanical properties of PCL-AT proved that it was not sufficient for bone repair. Therefore, in this study, HA or bone extracellular matrix powder (BP) was used to optimize the mechanical properties of PCL-AT matrices, and the effects were examined by a micro-CT analysis, while the improvement of the osteogenic activity by rabbit bone marrow MSCs was evaluated by gene expression analysis, MTS proliferation assay and an Alizarin Red functionality test.

Materials and methods

Preparation of PCL scaffolds by the phase separation technique. As previously reported (9), porous scaffolds were prepared using PCL (molecular weight ~65 kDa; density, 1.145 g/cm^3) (Sigma Chemical Co., St. Louis, MO, USA) and Ca^{2+} alginate threads at 200/100 weight ratio (Ca^{2+} alginate/PCL). To increase mechanical resistance and osteogenic properties, mineral components, such as HA or BP were added (PCL-AT-HA, PCL-AT-BP). In parallel, PCL without porogen (PCL-WP) was used as the control.

Hydroxyapatite. HA was prepared using calcium acetate aqueous solution [$Ca(Ac)_2$] (1 M) and ammonium phosphate aqueous solution [$(NH_4)\ H_2PO_4$] (1 M) as follows: 5 Ca $(Ac)_2$ + 3 $(NH_4)\ H_2\ PO_4$ + 7 (NH_4) (OH) → $Ca_5\ (PO_4)_3$ (OH) + 6 H_2O + 10 (NH_4) (Ac). The final solution pH was corrected to 10 with 33% ammonium hydroxide solution. The mixture was stirred for 24 h and then heated at 70˚C for 20 h under agitation. The resulting precipitate was filtered, washed and dried overnight.

Bone extracellular matrix powder. BP was obtained using the femurs of Sprague Dawley rats under animal care committee authorization. Following the removal of residual covering tissues, the samples were frozen in liquid nitrogen and pulverized using a mill. The resulting powder was treated with 0.5 M HCl solution (25 mEq/g) for 2 h at 4˚C and then centrifuged at 4˚C for 4 min at 4,000 rpm. To remove cellular contaminants from BP, 4 repeated cycles of detergent-enzymatic treatment were performed, as previously described by Meezan *et al* (19), each one consisting of the 3 following steps: i) distilled water for 72 h at 4˚C; ii) 4% sodium deoxycholate solution for 4 h; and iii) 2,000 KU DNase I in 1 M NaCl for 2 h.

Preparation of composite scaffolds. HA and BP were added to the PCL gel using 25/100 (PCL-AT-HA) and 13.3/100 (PCL-AT-BP) weight ratios, respectively. The samples were kept at 30˚C until complete solidification. The residual solvent and Ca^{2+} alginate threads were removed by washing with a sodium phosphate solution (0.1 M, pH 7.0) and then with distilled water.

Scaffold characterization

Morphological analysis. The size and distribution of pores were examined in the PCL matrices by scanning electron microscopy (SEM). The specimens were lyophilized, frozen in liquid nitrogen, fractured, coated with gold and observed using a Stereoscan-205 S scanning electron microscope (Cambridge Instruments, Cambridge, MA, USA).

Porosity measurement. The total porosity of the PCL scaffolds was determined by micro-CT analysis and density measurement, as previously described (9). Parallel sections were manually prepared and then scanned using a Skyscan 1172 HR Micro-CT scanner (Skyscan, Aartselaar, Belgium) using the following settings: voltage, 48 kV; current, 167 μA; exposition time, 363 msec; field of view (FOV), 1280x1024 pixels; and an 8-μm isotropic voxel size. Moreover, all samples were submitted to 360˚ rotation, a 0.4˚ rotation step and 1 frame averaging. The reconstruction of raw data was performed using N-Recon software (Skyscan) and a back projection algorithm was applied to the subsequent axial images acquired in bitmap format. Micro-CT images were analyzed using Ct-An software (Skyscan) and focusing the selected volume of interest (VOI; 3x1.59 mm) in the centre of each scaffold to prevent artifacts from cutting. All samples were binarized with the same instrument settings. Sample porosity was calculated as follows: $\Phi = 1 - BV/TV$, where Φ is total porosity, BV the bone volume, TV the total volume and BV/TV the percentage bone volume. Trabecular thickness (Tb.Th) (or pore wall) and trabecular separation (Tb.Sp) (or pore diameter) were computed by direct measurements. A 3D reconstruction was performed using CT Vol software (Skyscan) and OsiriX open-source software.

Biological properties of PCL scaffolds. The PCL scaffolds were sterilized in 95% ethanol for 2 h, incubated in PBS containing 2% penicillin/streptomycin solution and then washed 3 times in αMEM (Invitrogen, Grand Island, NY, USA). The scaffolds were then placed in 24-well plates, seeded with MSCs (3x10^4 cells/cm^2) and cultured in proliferative medium containing αMEM, 15% fetal bovine serum (FBS) (Invitrogen), 2 mM glutamax (Invitrogen) and 1% antibiotic solution (Sigma). At different time points, the samples were submitted to an analysis of cell viability study morphological analysis by SEM. To determine the effects of PCL matrices on osteogenic differentiation, the samples were cultured in differentiation and proliferative medium and subsequently analyzed by RT-PCR and functionality tests.

Mesenchymal stem cells. MSCs were isolated in sterile conditions from femurs and tibia of rabbits (rMSCs) acquired from private animal breeding. Following the removal of bone tips, bone marrow was harvested using Dulbecco's modified Eagle's medium (DMEM) (Invitrogen) supplemented with 0.2% penicillin-streptomycin (Invitrogen). The mononuclear cell fraction was then isolated by centrifugation (2,000 rpm, 30 min) on Ficoll 1077 (Invitrogen) density gradient and subsequently cultured in proliferative medium at 37˚C, 95% humidity and 5% CO_2. The immunophenotypical profile of bone marrow MSCs was verified on all primary cultures by detecting the expression of CD105, CD44, CD29, CD90, CD34 and CD45 by flow cytometry (FACS). The analysis was performed by indirect labeling using specific anti-rabbit primary antibodies and FITC-conjugated secondary antibodies (all from Santa

Table I. Primers used for RT-PCR.

Gene	Forward primer sequence (5'→3')	Reverse primer sequence (3'→5')
β-actin	AGATCTGGCACCACACCTTCTACA	ACTCGTCATACTCCTGCTTGCTGA
Runx2	AGTTTGTTCTCTGACCGCCTCAGT	ATGGTCGCCAGACAGATTCATCCA
Osteocalcin (OC)	CATGAGAGCCCTCACA	AGAGCGACACCCTAGAC
Osteopontin (OPN)	CCGACCAAGGAACAAT	CTCTGAAGCACCAGGATA
Collagene type I (Coll I)	GGCAAACATGGAAACCG	TCAAGGAAGGGCAAACG

Cruz Biotechnology, Inc., CA, USA). Samples were loaded on a FACSCanto II cytometer (BD Biosciences, San Jose, CA, USA) and the data were presented as a percentage of positive cells relative to the labeling control.

SEM. SEM was performed to evaluate the morphology and distribution of rabbit MSCs on the PCL scaffolds. At each time point (24 h, 7 and 14 days), the samples were washed with PBS and fixed with 3% glutaraldehyde in 0.1 M sodium cacodylate buffer (pH 7.4), for 24 h, at 4˚C. The specimens were then rinsed 3 times with sodium cacodylate buffer and dehydrated through a graded series of ethanol and then air-dried. The scaffolds were coated with gold and observed by SEM.

Analysis of cell viability. After seeding on PCL scaffolds, cell viability was monitored at 24 h, 72 h, 7 and 14 days using the colorimetric 3-(4,5-dimethylthiazol-2-yl)-5-(3-carboxymethoxyphenyl)-2-(4-sulfophenyl)-2H-tetrazolium (MTS) assay. Metabolically active cells react with tetrazolium salt in MTS reagent to produce a soluble formazan dye detectable at 490 nm. At each time point, all constructs were rinsed with PBS and then incubated for 3 h with 20% MTS reagent in culture medium. Thereafter, the aliquots were pipetted into 96-well plates and the absorbance of each sample was read at 490 nm using ELx 808 Ultra Microplate reader (Bio-Tek Instruments, Winooski, VT, USA). The data were expressed as the number of cells $x10^3$. A calibration curve (cell number/cm^2=$3.8x10^5A^{490}$-$1.1x10^4$, R^2=0.98) was prepared.

Osteogenic differentiation of MSCs on PCL matrices. At 48 h after seeding in proliferative medium, the cells were stimulated from 7 to 21 days with αMEM, 10% FBS, 1% antibiotic solution (APS), 0.1 μM dexamethasone, 10 nM β-glycerophosphate and 0.05 mM ascorbate. Cultures of MSCs in proliferative medium were used as the control. To verify the maturation into osteoblastic-like cells, all samples were submitted at different time points to the analysis of osteogenic markers by RT-PCR (7 and 14 days), alkaline phosphatase (ALP) activity analysis and the analysis of extracellular matrix calcium deposition by Alizarin Red staining (24 h, 7 and 14 days) as follows:

i) RT PCR. After 7 and 14 days, the constructs were rinsed with PBS and then submitted to total RNA extraction using TRIzol (Invitrogen). RNA was firstly quantified using a NanoDrop 2000 spectrophotometer (Thermo Scientific, Waltham, MA, USA) at 260 and 280 nm, and then reverse transcribed into cDNA by M-MLV Reverse Transcriptase (Sigma Aldrich), according to the manufacturer's instructions. For PCR amplification, ReadyMix™ Taq PCR Reaction Mix with $MgCl_2$ (Sigma) and specific oligo primers (Invitrogen) designed on GenBank sequences (Table I) were used. PCR products were then analyzed on 2% agarose gels and visualized using a Gel Doc imaging system (Bio-Rad, Hercules, CA, USA) after GelRed staining. The expression of β-actin was used as an internal control.

ii) Alkaline phosphatase assay. ALP activity was analyzed using p-nitrophenyl phosphate (p-NPP) as the substrate. Following cell lysis and centrifugation at 12,000 x g for 10 min, the supernatants were incubated with p-NPP for 30 min at 37˚C. The reaction was terminated by the addition of 3 N NaOH and the absorbance was measured at 405 nm. All results were expressed as the mean values ± SD of 3 separate experiments consisting of triplicates.

iii) Alizarin Red staining. To detect the calcium deposition of MSCs on the PCL scaffolds, an Osteogenesis assay kit (Millipore, Billerica, MA, USA) was used. The samples were fixed with 10% formalin solution for 15 min, washed twice with distilled water and then incubated with Alizarin Red S for 20 min at room temperature. After washing with distilled water and incubation for 30 min with 10% acetic acid under agitation, the cellular monolayers were then transferred to microcentrifuge tubes, heated to 85˚C for 10 min, placed on ice for 5 min and then centrifuged at 20,000 rpm for 15 min. After the addition of ammonium hydroxide, the amount of extracted Alizarin Red dye was measured at 562 nm and quantified using an Alizarin Red S standard curve. All results were expressed as the mean concentration (μM) ± SD of 3 separate experiments performed in triplicate on stimulated and unstimulated samples with osteogenic factors.

Statistical analysis. Data are expressed as the means value ± SD of at least 3 different samples. Significant differences were estimated by one-way analysis of variance (ANOVA) followed by a Student-Newman-Keuls post hoc test. Values of $p<0.05$ were considered to indicate statistically significant differences.

Results

PCL scaffolds. The absence of alginate threads in PCL-WP (Fig. 1A) determined a random formation of fine and not interconnected micropores. Homogeneously distributed pores largely characterized by a diameter of ~10 μm were observed by SEM in PCL-AT (Fig. 1B) and PCL-AT-BP (Fig. 1D) or ranging from 10 to 100 μm in PCL-AT-HA (Fig. 1C). Differently sized and distributed large pores due to air bubbles were detected in all samples.

Micro-CT analysis. The analysis revealed a significative increase in total porosity (Table II), trabecular spacing (Tb. Sp) (Fig. 2B) and trabecular thickness (Tb.Th) (Fig. 3B). In comparison to PCL-WP (Fig. 2A) characterized by a pore diam-

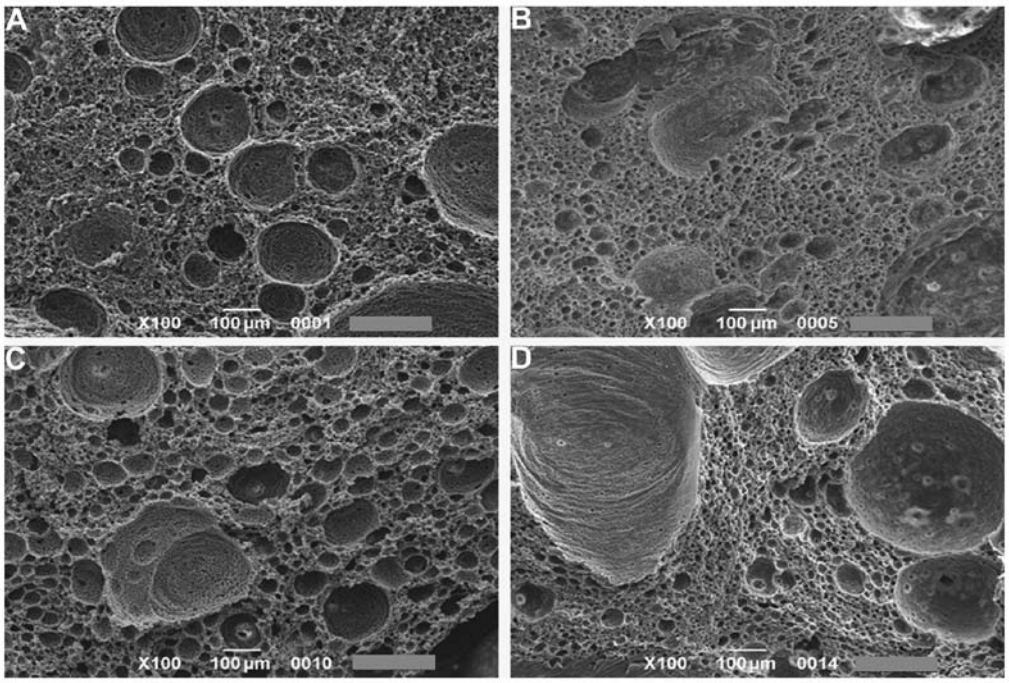

Figure 1. Pore distribution analysis by SEM on (A) PCL-WP, (B) PCL-AT, (C) PCL-AT-HA and (D) PCL-AT-BP scaffolds (magnification, x100). PCL, poly-ε-caprolactone; WP, without porogen; AT, alginate threads; AT-HA, alginate threads and hydroxyapatite; AT-BP, alginate threads and bone powder.

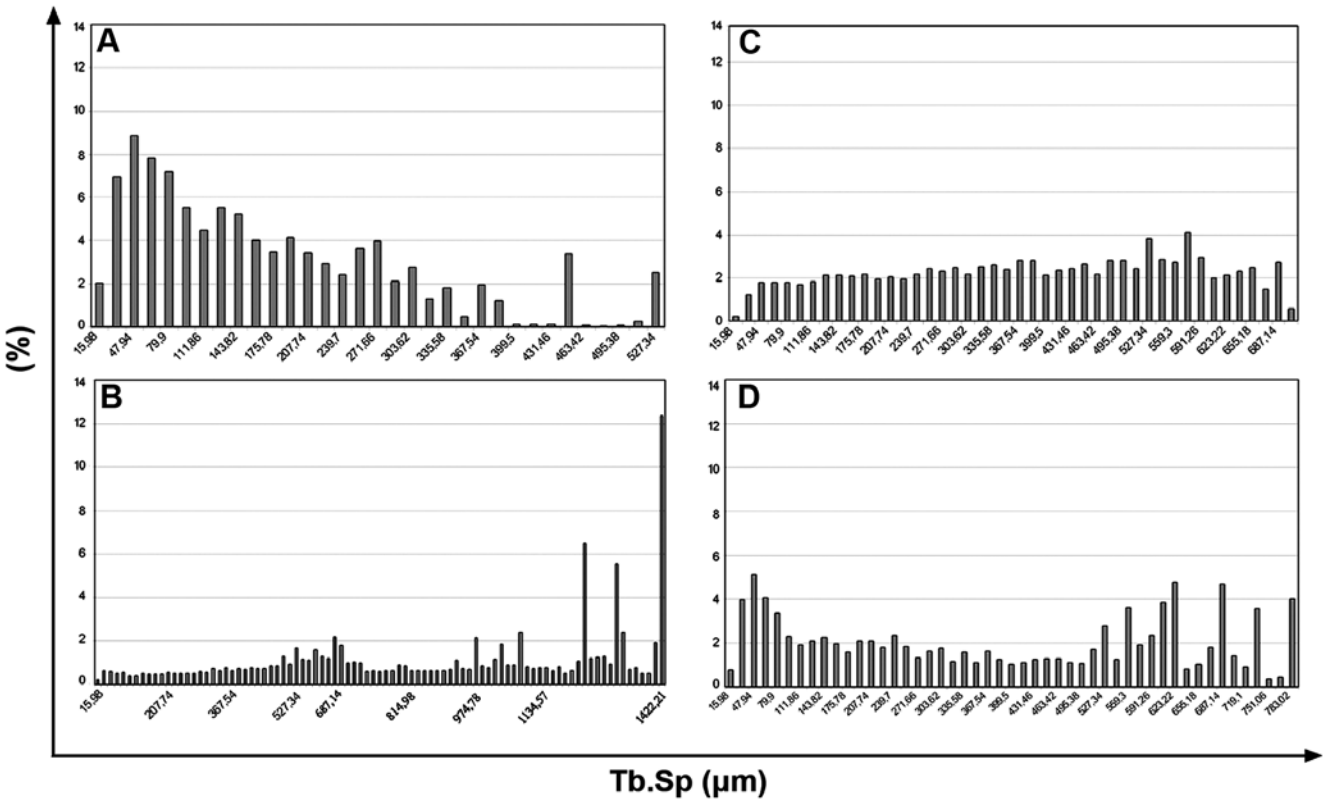

Figure 2. Measurement of trabecular separation (Tb.Sp) by micro-CT on (A) PCL-WP, (B) PCL-AT, (C) PCL-AT-HA and (D) PCL-AT-BP scaffolds. Data were computed by direct measurements. PCL, poly-ε-caprolactone; WP, without porogen; AT, alginate threads; AT-HA, alginate threads and hydroxyapatite; AT-BP, alginate threads and bone powder.

eter ranging from ~15 to 300 μm, PCL-AT (Fig. 2B) showed a porous structure with cavities homogeneously distributed and sized (diameter, ~15 to 1,400 μm). In PCL-AT-HA (Fig. 2C) and PCL-AT-BP (Fig. 2D), the maximum size of the pores detected was ~700 μm and unimodal (Fig. 2C) or bimodal (Fig. 2D) distribution was respectively observed. In parallel, Tb.Th values ranging from ~15 to 600 μm were observed with a similar distribution in PCL-AT (Fig. 3B) and PCL-AT-BP (Fig. 3D) in

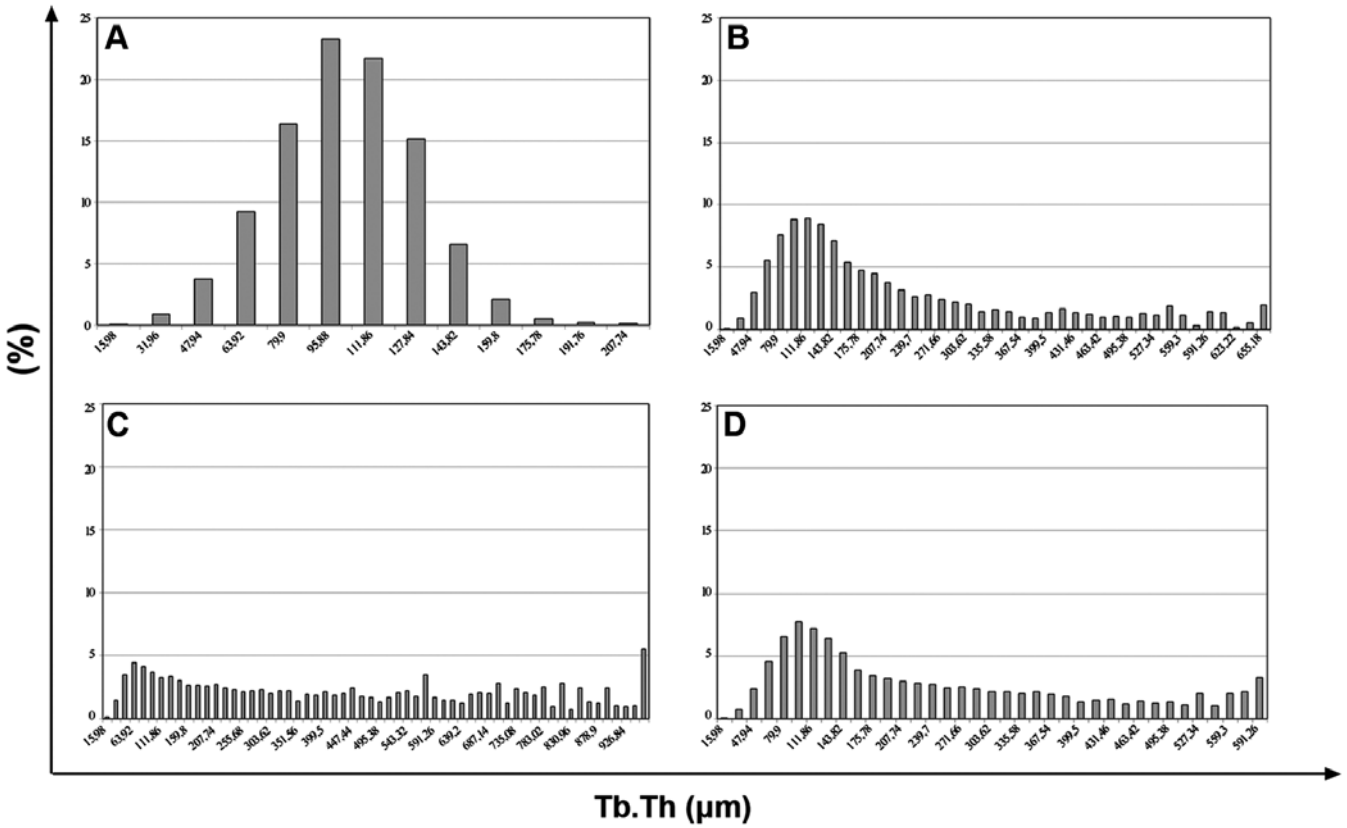

Figure 3. Micro-CT analysis of trabecular thickness (Tb.Th) on (A) PCL-WP, (B) PCL-AT, (C) PCL-AT-HA and (D) PCL-BP scaffolds. Data were computed by direct measurements. PCL, poly-ε-caprolactone; WP, without porogen; AT, alginate threads; AT-HA, alginate threads and hydroxyapatite; AT-BP, alginate threads and bone powder.

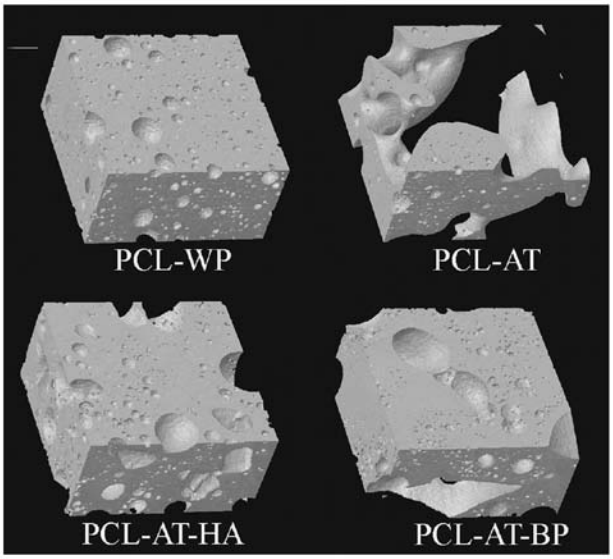

Figure 4. 3D reconstruction of PCL scaffolds by micro-CT analysis. PCL, poly-ε-caprolactone; WP, without porogen; AT, alginate threads; AT-HA, alginate threads and hydroxyapatite; AT-BP, alginate threads and bone powder.

Table II. Total porosity value of PCL matrices detected by micro-CT analysis and density measurement.

Samples	Φ micro-CT (% value ± SD)	Φ density method (% value ± SD)
PCL-WP	21.59±7.06	70±3.75
PCL-AT	51.83±5.30	79.6±1.17
PCL-AT-HA	55.92±5.31	82.5±0.46
PCL-AT-BP	52.53±3.15	84±0.43

PCL, poly-ε-caprolactone; Φ, total porosity; SD, standard deviation; WP, without porogen; AT, alginate threads; AT-HA, alginate threads and hydroxyapatite; AT-BP, alginate threads and bone powder.

comparison to the control characterized by Tb.Th values from ~15 to 150 μm (Fig. 3A). The highest Tb.Th value (~900) was observed in PCL-AT-HA (Fig. 3C). 3D scaffold reconstruction confirmed the presence of interconnected pores in all scaffolds relative to the control (Fig. 4), suggesting a trabecular bone-like structure. As shown in Fig. 5, the addition of HA did not significantly alter the mechanical properties of PCL-AT. An increase in the displacement value (3,900±2.17) and the shift/deformation due to the load (3,273±4.73) observed on PCL-AT-BP suggested that the addition of BP led to a reduction in the elastic module of the PCL-AT matrix, preserving the porous structure.

Biological properties of PCL scaffolds

MSC cultures. A total of 7 days after seeding, typical colony forming units with fibroblastic cell morphology (Fig. 6A) were observed. FACS analysis revealed that the rMSCs were

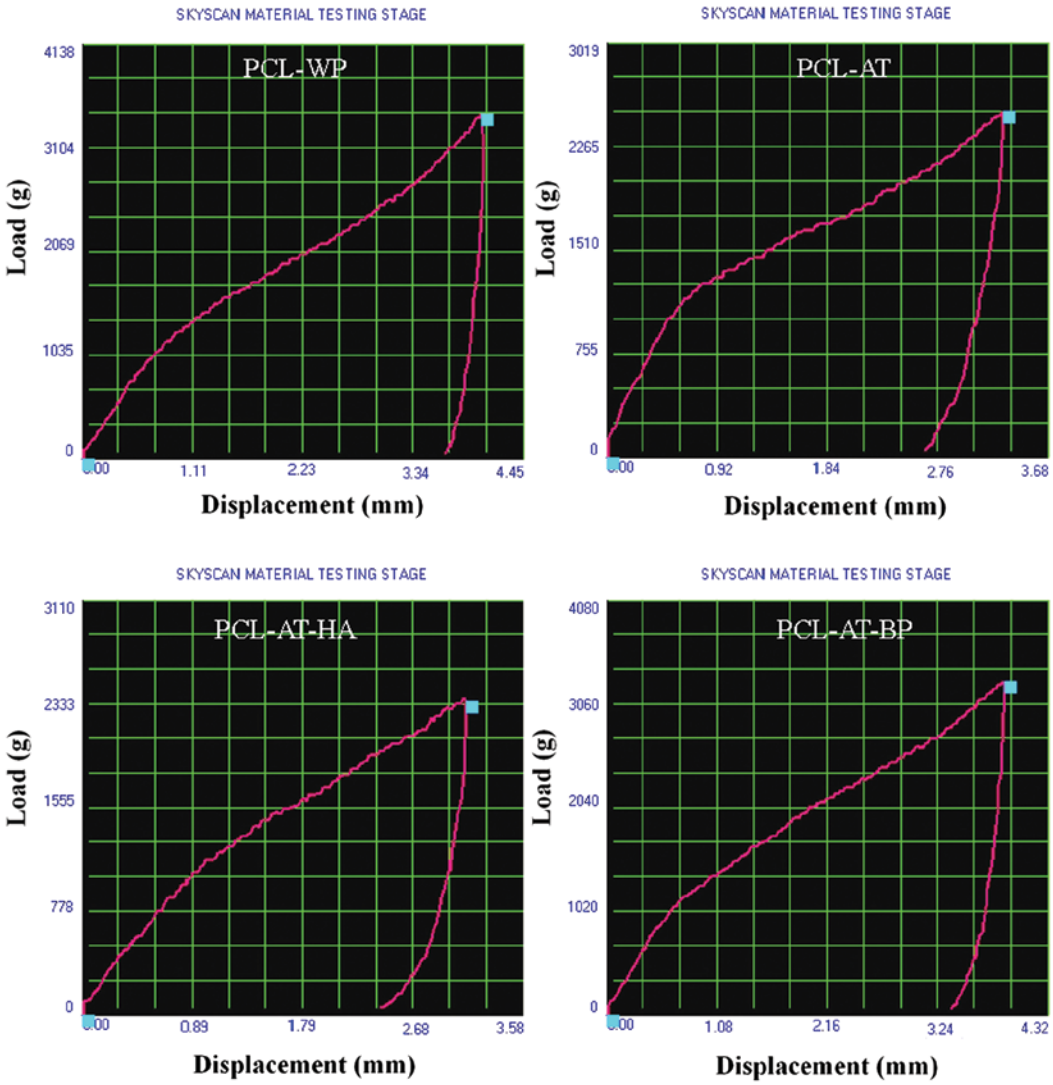

Scaffolds	Displacement (mm) (average±SD)	Load (g) (average±SD)
PCL-WP	4030 ± 3.55	3438 ± 4.75
PCL-AT	3310 ± 5.53	2516 ± 3.98
PCL-AT-HA	3110 ± 2.74	2347 ± 3.73
PCL-AT-BP	3900 ± 2.17	3273 ± 4.73

Figure 5. Loading displacement test performed by micro-CT analysis on PCL scaffolds. Data from 3 independent experiments were acquired using the SkyScan Material testing stage and are expressed as the average values of 3 experiments ± standard deviation (SD). PCL, poly-ε-caprolactone; WP, without porogen; AT, alginate threads; AT-HA, alginate threads and hydroxyapatite; AT-BP, alginate threads and bone powder.

positive for MSC markers, such as CD105, CD44, CD29 and CD90 and negative for hematopoietic markers, such as CD34 and CD45 (Fig. 6B).

MTS assay. From 24 h to 14 days, porous PCL matrices showed a significant increase in cell viability relative to the control (Fig. 8). Larger cavities were shown to promote optimal

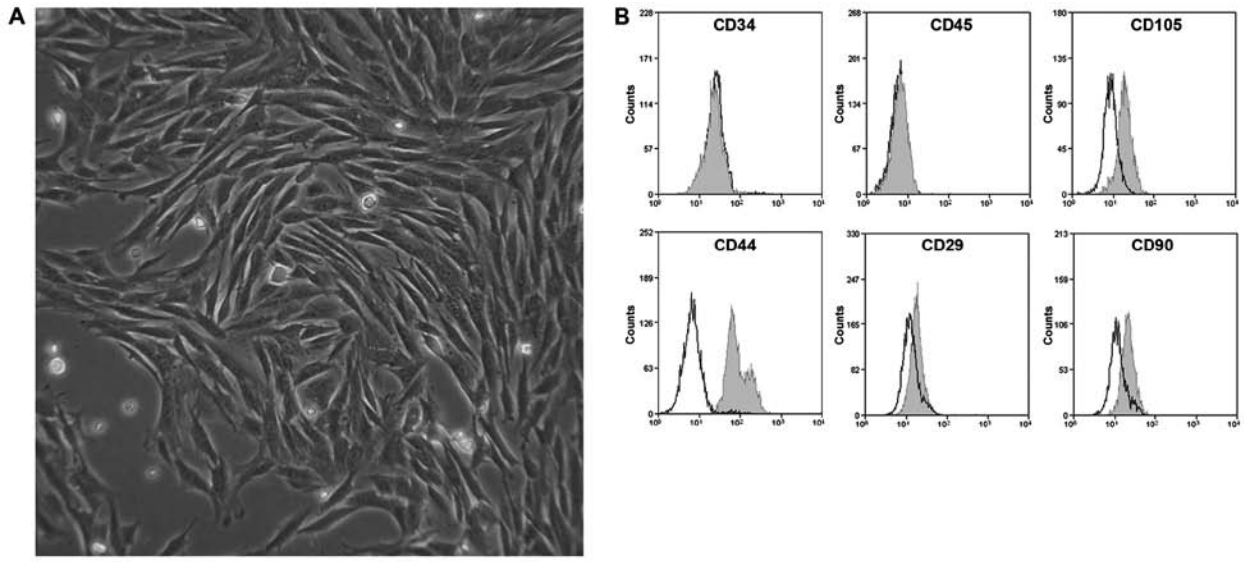

Figure 6. (A) Contrast phase microscopy of MSC primary cultures isolated from rabbit bone marrow (rMSCs) (magnification, x100). (B) Immunophenotypical characterization of rMSCs by FACS. Data from samples treated with anti-rabbit CD34, -CD45, -CD105, -CD44, -CD29 and -CD90 antibodies (grey peak) were compared to the controls (black peak) labeled only with FITC-conjugated secondary antibody.

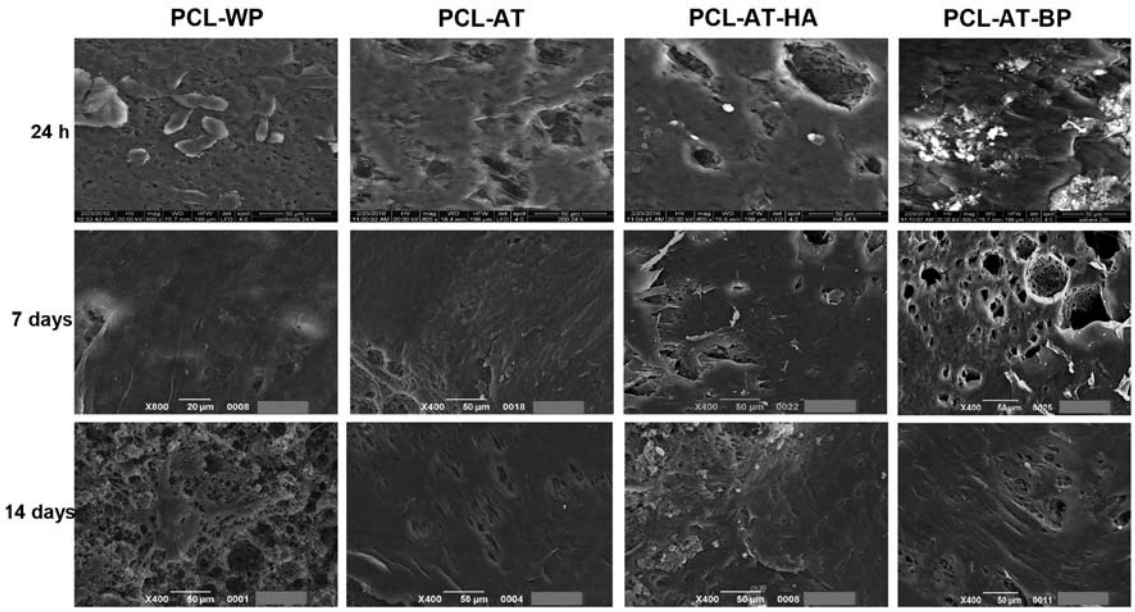

Figure 7. SEM micrographs of rabbit MSCs (rMSCs) grown on PCL matrices (magnification, x400). PCL, poly-ε-caprolactone; WP, without porogen; AT, alginate threads; AT-HA, alginate threads and hydroxyapatite; AT-BP, alginate threads and bone powder.

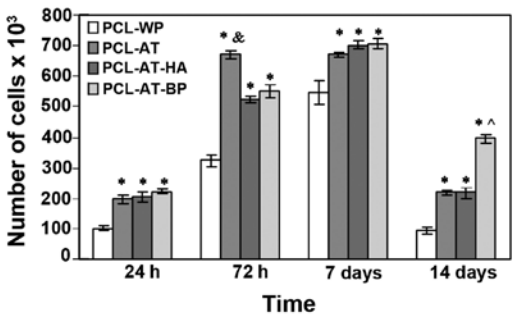

Figure 8. Analysis of the viability of rabbit MSCs (rMSCs) cultured on PCL matrices for 2 weeks by MTS assay. *p<0.05 vs. PCL-WP at each time point; &p<0.05 vs. PCL-AT-HA and PCL-AT-BP; ^p<0.05 vs. PCL-AT and PCL-AT-HA. PCL, poly-ε-caprolactone; WP, without porogen; AT, alginate threads; AT-HA, alginate threads and hydroxyapatite; AT-BP, alginate threads and bone powder.

conditions for cell growth at 72 h, as detected in PCL-AT. After 1 week, all porous PCL scaffolds presented similar cell proliferation rates ($p<0.05$) in comparison to PCL-WP (Fig. 8). Although cell viability markedly decreased in all samples at 14 days, possibly due to an impaired flux of nutrients and gas under static growth conditions, the cell number detected on PCL-BP significantly ($p<0.05$) diverged from that of the control, suggesting that the porosity grade and BP prolonged the cell viability on the PCL scaffolds over time.

SEM. At 24 h after cell seeding, the surface of all the porous PCL scaffolds was shown to be largely populated by MSCs (Fig. 7). From 7 to 14 days, the cells were still organized in a monolayer. By contrast, the rare cells observed on

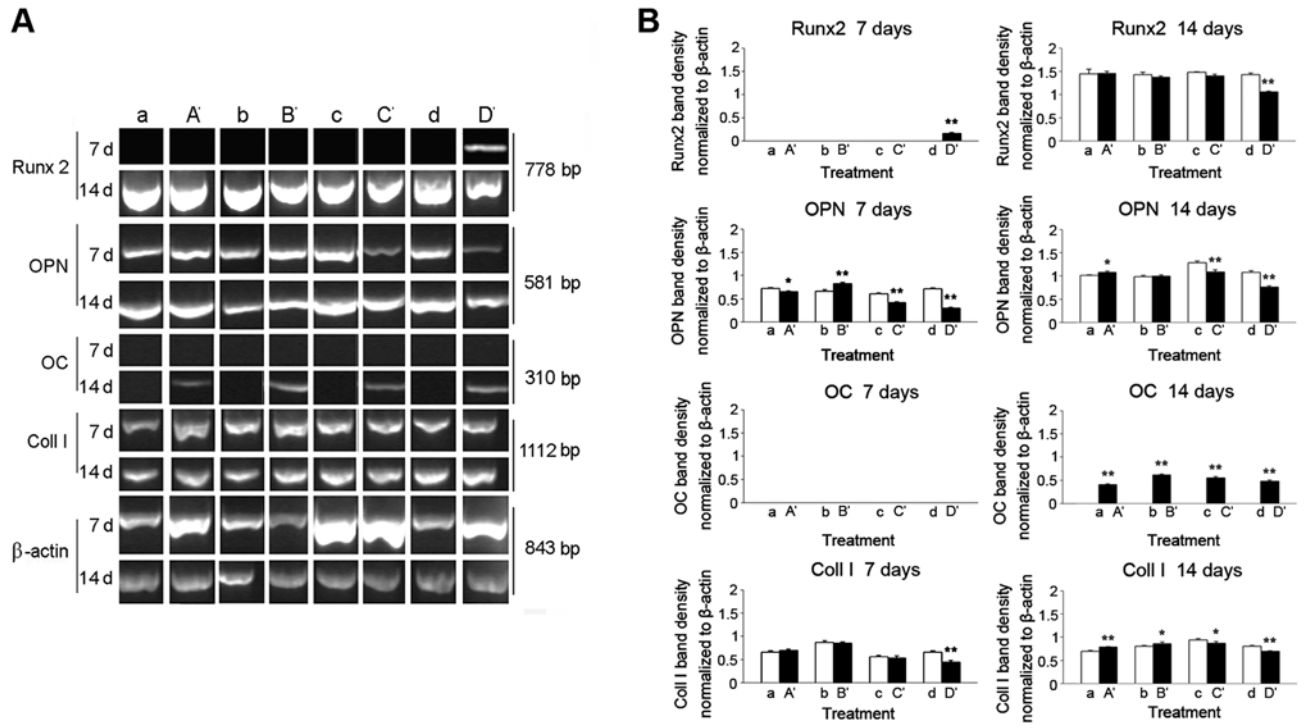

Figure 9. (A) Expression of Runx2, osteopontin (OPN), osteocalcin (OC) and collagen I (Coll I) mRNAs in MSCs cultured for 7 (7d) and 14 days (14d) in (a-d) proliferative and (A'-D') osteogenic medium on (a, A') PCL-WP, (b, B') PCL-AT, (c, C') PCL-AT-HA and (d, D') PCL-AT-BP scaffolds. In parallel, the gene expression of the housekeeping, β-actin, was evaluated. All RT-PCR products were electrophoresed on 2% agarose gels pre-stained with GelRed. (B) Densitometry of agarose gel bands. $^{*}p<0.05$; $^{**}p<0.01$. PCL, poly-ε-caprolactone; WP, without porogen; AT, alginate threads; AT-HA, alginate threads and hydroxyapatite; AT-BP, alginate threads and bone powder.

PCL-WP at the early (24 h), intermediate (7 days) and late growth phase (14 days) suggested that the scaffold porosity grade was not functional to guarantee cell viability, adhesion and proliferation.

RT-PCR. The expression of osteopontin (OPN) and Coll I was shown to be independent of PCL substrates (Fig. 9). Although its expression was detected at 14 days in the samples under both proliferative and osteogenic conditions, Runx2 was expressed as early as 7 days on PCL-BP, possibly due to the combined stimulatory effects of the composite matrix and differentiation medium. Independent of the porosity grade of the scaffolds, the differentiation induction by soluble factors was shown to strictly control the mRNA expression of osteocalcin (OC) in rMSCs (Fig. 9A-D).

ALP assay and Alizarin Red staining. From 24 h to 14 days, a low activity of the ALP enzyme was detected in all porous PCL scaffolds and control samples under proliferative conditions (Fig. 10A). When the MSCs were induced with osteogenic medium, the ALP value significantly ($p<0.05$) increased. In particular, the differentiated cells on PCL-HA (7 days) and PCL-BP (7, 14 days) showed a significant ($p<0.05$) increase in ALP activity in comparison to PCL-AT, suggesting that BP and HA enhanced the osteogenic properties of the porous PCL scaffolds. As expected, mineralized deposits (Fig. 10B) were detected from 24 h to 14 days on PCL-HA under both proliferative ($p<0.05$) and differentiation ($p<0.05$) conditions. The BP extracts revealed to be effective ($p<0.05$) in stimulatig ECM mineralization from 7 to 14 days only in samples cultured in osteogenic medium.

Discussion

Following bone injury, the healing process develops through the recruitment of immature cells that first originate from osteoprogenitor cells (20) and then differentiate into bone cells under local, biochemical and biophysical stimuli. During bone implant incorporation, the phenomenon of osteoinduction can be observed (20). It is dependent on scaffold properties, such as porosity, which is defined as the percentage of internal void space (21) and pore size (22). Including micropores (diameter size <10 μm) and macropores (diameter size >50 μm), total porosity is a variable parameter among tissue sites (~50-90% in trabecular bone and 3-12% in cortical tissue) (23,24) and is crucial for the invasive growth of cells, vascularization and the diffusion of nutrients and gasses. Thus, for bone replacement, in order to achieve optimal bone-tissue outcomes, the effects of pore size and morphology on osteoinduction and scaffold mechanical properties have been extensively investigated (25,26). As large pores favour direct osteogenesis and small pores guarantee osteochondral ossification, fabricating scaffolds with different grades of porosity and pore size is appealing in terms of improving the bone regeneration process.

Grandi *et al* (9) demonstrated that the biological activities of PCL scaffolds obtained by the phase separation technique were greatly enhanced when alginate threads were added as the porogen (PCL-AT) and pore size was in the range of 15-1,400 nm. As a bigger void volume implies a reduction in scaffold mechanical strength, and the tensile strength of PCL-AT was not optimal for *in vivo* bone applications, in the present study,

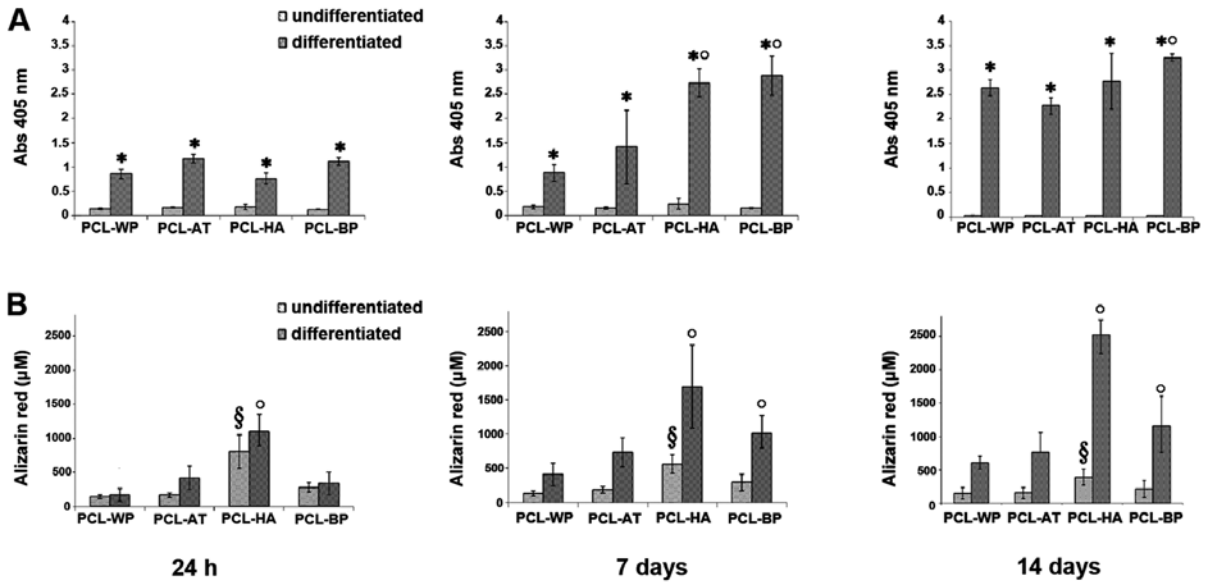

Figure 10. Alkaline phosphatase assay (A) and Alizarin red staining (B) of rabbit MSCs (rMSCs) grown on PCL scaffolds in proliferative and differentiation medium for 24 h, 7 and 14 days. *p<0.05 vs. corresponding undifferentiated sample; °p<0.05 vs. differentiated PCL-WP; §p<0.05 vs. undifferentiated PCL-WP. PCL, poly-ε-caprolactone; WP, without porogen; AT, alginate threads; AT-HA, alginate threads and hydroxyapatite; AT-BP, alginate threads and bone powder.

mineral components, such as HA or decellularized bone matrix powder (BP) were used in order to prepare composite PCL-AT matrices with increased mechanical strength. The obtained multi-scale porosity and pore size in the range of ~15-800 nm in both PCL-AT-HA and PCL-AT-BP was in agreement with structural properties previously reported as functional to promote *in vivo* bone regeneration. In particular, Hulbert *et al* (21) demonstrated that pore sizes in the range of 100-150 and 150-200 μm resemble normal haversian systems and stimulate *in vivo* substantial bone ingrowth. Macropores with a diameter of 400-600 μm in porous HA implants have been shown to promote the *in vivo* healing of rat femoral defects (27), while pores ranging from 100 to 600 μm have been shown to sustain the *in vitro* osteogenic differentiation of murine pluripotent C3H10T1/2 cells (28).

As the *in vivo* bone environment is subjected to mechanical compression, an elective scaffold for bone regeneration must be designed to withstand this force, while adequate porosity [Bignon *et al* (29)] is preserved. In the present study, the porous PCL-AT scaffold demonstrated a significant increase in structural resistance only when decellularized extracellular bone matrix was added, suggesting that the reduction of total macropores due to HA is not sufficient to modify the scaffold structural strength. Despite being characterized by a high level of osteoconductivity, HA is considered a bone graft extender or carrier of growth factors rather than a 'stand-alone' bone graft substitute. It is weak in tensile strength and toughness, and thus when added to bone scaffolds, no significant change in mechanical properties was detected while, as expected, a reduction in total porosity, trabecular thickness and trabecular space was observed.

As previously reported (9) and confirmed in this study, the adhesion and proliferation of bone-forming cells in PCL-AT scaffolds are enhanced by pores differentially organized into 'blind', 'closed' and 'through' pores (30). 'Blind' pores start from one surface and terminate inside the material. They influence the amount of fluids that can be stored within a matrix and contribute to increasing the surface area of cell growth. 'Closed' pores are void cavities not connected to the external surface and do not contribute to the inflow of nutrients and gasses. 'Through' pores are channels extending from one free scaffold surface to another and are responsible for the flow of fluid through the material. Although the role of porosity in bone substitution to promote the migration and proliferation of osteoblasts and mesenchymal cells, as well as vascularization (31) has been demonstrated, the optimal porosity percentage and pore size have been not yet been identified. In this study, we demonstrated that the increased porosity of scaffolds due to AT was associated with a major degree of cell adhesion and proliferation. Moreover, the heterogeneity of scaffold pores in PCL-AT-HA and PCL-AT-BP was shown to favour the growth and differentiation of MSCs isolated from rabbit bone marrow.

The proliferation of osteoblasts and mesenchymal cells has been largely demonstrated to be dependent on both macropores, assuring a major interconnected network of void cavities and an improved oxygen and nutrients inflow (31-33), as well as micropores, stimulating high levels of bone-inducing protein adsorption, ion exchange and bone-like apatite formation (34). Although the greater porosity in PCL-AT guaranteed better conditions for the proliferation of MSCs at the early phase, the presence of BP was shown to be crucial to prolong the viability of cells at the late phase.

It is known that the microenviroment and soluble factors interact to drive the proliferation and differentiation of cells. When rMSCs were cultured for 14 days on porous PCL scaffolds, the mRNA expression of Coll I and OPN was observed at the early and late phase suggesting their expression is not controlled by the microenviroment. The mRNA expression of Runx2 (at 7 days) and osteocalcin (at 14 days) was observed only following stimulation with osteogenic factors, demonstrating that soluble factors cooperate with the microenviroment to promote the progression of the differentiation process. The transcription factor, Runx2, is a key regulator of osteoblast differentiation (35), controlling both intramembranous and endochondral bone formation (36)

and promoting chondrocyte maturation (37). As the expression of Runx2 progressively increased during osteogenic differentiation, and the activity of ALP and the levels of osteocalcin in the culture-expanded MSCs significantly increased in response to Runx2, it can be hypothesized that all porous PCL scaffolds sustain the expression of certain osteogenic markers, but only in combination with specific inducers (HA or BP) and that they are functional to promote the activity of ALP and the mineralization of ECM, suggesting a marked influence of HA and BP on osteogenic maturation in bone substitutes.

In conclusion, the data presented in this study indicate that PCL scaffolds prepared with AT as the porogen and HA or BP acquire similar osteoinductive properties, but differ in mechanical strength. Due to the more appropriate porosity grade, structural resistance and biological properties, PCL-AT-BP was shown to have greater potential for use in bone repair applications.

Acknowledgements

We would like to thank San Luca Hospital, ULSS 18, Trecenta (Rovigo), Italy and the University of Padua for providing the laboratory facilities. We would also like to express our gratitude to Thomas Bertalot for providing technical support.

References

1. Tabata Y: Biomaterial technology for tissue engineering applications. J R Soc Interface 6 (Suppl 3): 311-324, 2009.
2. Porter JR, Ruckh TT and Popat KC: Bone tissue engineering: a review in bone biomimetics and drug delivery strategies. Biotechnol Prog 25: 1539-1560, 2009.
3. Langer R and Vacanti JP: Tissue engineering. Science 260: 920-926, 1993.
4. Schmitz JP and Hollinger JO: A preliminary study of the osteogenic potential of a biodegradable alloplastic-osteoinductive alloimplant. Clin Orthop Relat Res 237: 245-255, 1988.
5. Mikos AG, Sarakinos G, Leite SM, Vacanti JP and Langer R: Laminated threedimensional biodegradable foams for use in tissue engineering. Biomaterials 14: 323-330, 1993.
6. Agrawal CM and Kennedy MB: The effects of ultrasound irradiation on a biodegradable delivery system. Transactions of the Society for Biomaterials 19: 292, 1993.
7. Mooney DJ, Baldwin DF, Suh NP, Vacanti JP and Langer R: Novel approach to fabricate porous sponges of poly (D,L-lactic-co-glycolic acid) without the use of organic solvents. Biomaterials 17: 1417-1422, 1996.
8. Schugens C, Maquet V, Grandfils C, Jerome R and Teyssie P: Polylactide macroporous biodegradable implants for cell transplantation. II. Preparation of polylactide foams by liquid-liquid phase separation. J Biomed Mat Res 30: 449-461, 1996.
9. Grandi C, Di Liddo R, Paganin P, Lora S, Dalzoppo D, Feltrin G, Giraudo C, *et al*: Porous alginate/poly(ε-caprolactone) scaffolds: preparation, characterization and *in vitro* biological activity. Int J Mol Med 27: 455-467, 2011.
10. Costa-Pinto AR, Reis RL and Neves NM: Scaffolds based bone tissue engineering: the role of chitosan. Tissue Eng Part B Rev17: 331-347, 2011.
11. Karsenty G: The genetic transformation of bone biology. Genes Dev 13: 3037-3051, 1999.
12. Ito Y, Hasuda H, Kamitakahara M, Ohtsuki C, Tanihara M, Kang IK and Kwon OH: A composite of hydroxyapatite with electrospun biodegradable nanofibers as a tissue engineering material. J Biosci Bioeng 100: 43-49, 2005.
13. Thomas V, Jagani S, Johnson K, Jose MV, Dean DR, Vohra YK and Nyairo E: Electrospun bioactive nanocomposite scaffolds of polycaprolactone and nanohydroxyapatite for bone tissue engineering. J Nanosci Nanotechnol 6: 487-493, 2006.
14. Teng SH, Lee EJ, Wang P and Kim HE: Collagen/hydroxyapatite composite nanofibers by electrospinning. Mater Lett 62: 3055-3058, 2008.
15. Ngiam M, Liao S, Patil AJ, Cheng Z, Chan CK and Ramakrishna S: The fabrication of nano-hydroxyapatite on PLGA and PLGA/collagen nanofibrous composite scaffolds and their effects in osteoblastic behavior for bone tissue engineering. Bone 45: 4-16, 2009.
16. Venugopal J, Low S, Choon AT, Sampath Kumar TS and Ramakrishna S: Mineralization of osteoblasts with electrospun collagen/hydroxyapatite nanofibers. J Mater Sci Mater Med 19: 2039-2046, 2008.
17. Woodward SC, Brewer PS, Moatamed F, Schindler A and Pitt CG: The intracellular degradation of poly (epsilon-caprolactone). J Biomed Mater Res 19: 437-444, 1985.
18. Phipps MC, Clem WC, Catledge SA, *et al*: Mesenchymal stem cell responses to bone-mimetic electrospun matrices composed of polycaprolactone, collagen I and nanoparticulate hydroxyapatite. PLoS One 6: e16813, 2011.
19. Meezan E, Hjelle JT, Brendel K and Carlson EC: A simple, versatile, nondisruptive method for the isolation of morphologically and chemically pure basement membranes from several tissues. Life Sci 17: 1721-1732, 1975.
20. Albrektsson T and Johansson C: Osteoinduction, osteoconduction andosseointegration. Eur Spine J 10 (Suppl 2): 96-101, 2001.
21. Hulbert SF, Young FA, Mathews RS, Klawitter JJ, Talbert CD and Stelling FH: Potential of ceramic materials as permanently implantable skeletal prostheses. J Biomed Mater Res 4: 433-456, 1970.
22. Karageorgiou V and Kaplan D: Porosity of 3D biomaterial scaffolds and osteogenesis. Biomaterials 26: 5474-5491, 2005.
23. Kaplan FS, Hayes WC, Keaveny TM, Boskey A, Einhorn TA and Iannotti JP: Form and function of bone. In: Orthopaedic Basic Science. Simon SR (ed). American Academy of Orthopaedic Surgeons, Rosemont, IL, pp127-185, 1994.
24. Cooper DM, Matyas JR, Katzenberg MA and Hallgrimsson B: Comparison of microcomputed tomographic and microradiographic measurements of cortical bone porosity. Calcif Tissue Int 74: 437-447, 2004.
25. Bauer TW and Muschler GF: Bone graft materials. An overview of the basic science. Clin Orthop Relat Res: 10-27, 2000.
26. Keating JF and McQueen MM: Substitutes for autologous bone graft in orthopaedic trauma. J Bone Joint Surg 83: 3-8, 2001.
27. Damien E, Hing K, SaeedS and Revell PA: A preliminary study on the enhancement of the osteointegration of a novel synthetic hydroxyapatite scaffold in vivo. J Biomed Mater Res A 66: 241-246, 2003.
28. Kim HD and Valentini RF: Retention and activity of BMP-2 in hyaluronic acid-based scaffolds in vitro. J Biomed Mater Res 59: 573-584, 2002.
29. Bignon A, Chouteau J, Chevalier J, Fantozzi G, Carret JP, Chavassieux P, Boivin G, Melin M and Hartmann D: Effect of micro- and macroporosity of bone substitutes on their mechanical properties and cellular response. J Mater Sci Mater Med 14: 1089-1097, 2003.
30. Ahuja G and Pathak K: Porous carriers for controlled/modulated drug delivery. Indian J Pharm Sci 71: 599-607, 2009.
31. Kuboki Y, Takita H, Kobayashi D, *et al*: BMP-induced osteogenesis on the surface of hydroxyapatite with geometrically feasible and nonfeasible structures: topology of osteogenesis. J Biomed Mater Res 39: 190-199, 1998.
32. Tsuruga E, Takita H, Itoh H, Wakisaka Y and Kuboki Y: Pore size of porous hydroxyapatite as the cell-substratum controls BMP-induced osteogenesis. J Biochem 1: 317-324, 1997.
33. Gotz HE, Muller M, Emmel A, Holzwarth U, Erben RG and Stangl R: Effect of surface finish on the osseointegration of laser-treated titanium alloy implants. Biomaterials 25: 4057-4064, 2004.
34. Yuan H, Kurashina K, de Bruijn JD, Li Y, de Groot K and Zhang X: A preliminary study on osteoinduction of two kinds of calcium phosphate ceramics. Biomaterials 20: 1799-1806, 1999.
35. Dong SW, Ying DJ, Duan XJ, *et al*: Bone regeneration using an acellular extracellular matrix and bone marrow mesenchymal stem cells expressing Cbfa1. Biosci Biotechnol Biochem 73: 2226-2233, 2009.
36. Komori T, Yagi H, Nomura S, *et al*: Targeted disruption of Cbfa1 results in a complete lack of bone formation owing to maturational arrest of osteoblasts. Cell 89: 755-764, 1997.
37. Inada M, Yasui T, Nomura S, *et al*: Maturational disturbance of chondrocytes in Cbfa1-deficient mice. Dev Dyn 214: 279-290, 1999.